

Gondwanide continental collision and the origin of Patagonia

R.J. Pankhurst^{1*}, C.W. Rapela², C.M. Fanning³, M. Márquez⁴

1. *Visiting Research Associate, NERC Isotope Geosciences Laboratory, British Geological Survey, Keyworth, Nottingham NG12 5GG, U.K.*

2. *Centro de Investigaciones Geológicas, CONICET-UNLP, Calle 1 No. 644, 1900 La Plata, Argentina*

3. *Research School of Earth Sciences, The Australian National University, Mills Road, Canberra, ACT 200, Australia*

4. *Universidad Nacional de la Patagonia San Juan Bosco, Departamento de Geología, Kilómetro 4, 9000 Comodoro Rivadavia, Argentina.*

*Corresponding author. Tel.: +44 115 9363263; fax.: +44 115 9363302.

E-Mail addresses: rjpt@nigl.nerc.ac.uk (R.J. Pankhurst), crapela@cig.museo.unlp.edu.ar (C.W. Rapela), mark.fanning@anu.edu.au (C.M. Fanning), marcelo28marquez@yahoo.com (M. Márquez).

Abstract

A review of the post-Cambrian igneous, structural and metamorphic history of Patagonia, largely revealed by a five-year programme of U–Pb zircon dating (32 samples), geochemical and isotope analysis, results in a new Late Palaeozoic collision model as the probable cause of the Gondwanide fold belts of South America and South Africa.

In the northeastern part of the North Patagonian Massif, Cambro-Ordovician metasediments with a Gondwana provenance are intruded by Mid Ordovician granites analogous to those of the Famatinian arc of NW Argentina; this area is interpreted as Gondwana continental crust at least from Devonian times, probably underlain by Neoproterozoic crystalline basement affected by both Pampean and Famatinian events, with a Cambrian rifting episode previously identified in the basement of the Sierra de la Ventana. In the Devonian (following collision of the Argentine Precordillera terrane to the north), the site of magmatism jumped to the western and southwestern margins of the North Patagonian Massif, although as yet the tectonics of this magmatic event are poorly

32 constrained. This was followed by Early Carboniferous I-type granites representing a
33 subduction-related magmatic arc and mid-Carboniferous S-type granites representing
34 crustal anatexis. The disposition of these rocks implies that the North Patagonian Massif
35 was in the upper plate, with northeasterly subduction beneath Gondwana prior to the
36 collision of a southern landmass represented by the Deseado Massif and its probable
37 extension in southeastern Patagonia. This ‘Deseado terrane’ may have originally rifted off
38 from a similar position during the Cambrian episode. Intense metamorphism and granite
39 emplacement in the upper plate continued into the Early Permian. Known aspects of Late
40 Palaeozoic sedimentation, metamorphism, and deformation in the Sierra de la Ventana and
41 adjacent Cape Fold Belt of South Africa are encompassed within this model. It is also
42 compatible with modern geophysical and palaeomagnetic data that do not support previous
43 hypotheses of southward-directed subduction and collision along the northern limit of
44 Patagonia. Subsequent Permian break-off of the subducted plate, perhaps with
45 delamination of the lower part of the upper plate, allowed access of heat to the overlying
46 Gondwana margin and resulted in voluminous and widespread silicic plutonism and
47 volcanism throughout Permian and into Triassic times. Thus the new model addresses and
48 attempts to explain three long-standing geological enigmas – the origin of the Gondwanide
49 fold belts, the origin of Patagonia, and the cause of widespread Permian silicic magmatism
50 (Choiyoi province) in southern South America. Differing significantly from previous
51 models, it has new implications for the crustal structure, mineral resources, and the plant
52 and animal distribution in this part of Gondwana, since the southern landmass would have
53 had an independent evolution throughout the Early Palaeozoic.

54

55

56 *Keywords:* Patagonia; Gondwana; Sierras Australes; Cape fold belt; continental collision; U–Pb zircon.

58 **1. Introduction**

59 Patagonia, conventionally considered as the continental region south of the Río
60 Colorado (Fig. 1), has long been recognized as differing from the rest of South America in
61 terms of its topography, environment, flora, fauna and palaeontological record. The idea
62 that it could have had a separate geological history (Keidel, 1925) was stimulated by the
63 recognition of terrane accretion processes in the early 1980s. Ramos (1984; 1986)
64 proposed that an allochthonous (exotic) Patagonian terrane collided with cratonic South
65 America (supercontinental Gondwana) along the Río Colorado zone in Carboniferous
66 times. In his model, the suture (obscured by much younger sediments) formed by closure
67 of a previously intervening ocean, due to southwest-dipping subduction beneath the North
68 Patagonian Massif. In more recent reviews of the tectonic evolution of Patagonia, Ramos
69 (2002, 2004) has modified this idea to include a prior Early Palaeozoic collision within the
70 Deseado Massif, also thought to result from southward-direct subduction, prior to Late
71 Palaeozoic collision of the combined landmass so formed with cratonic South America, as
72 before. In partial support of these models, Devonian–Carboniferous penetrative
73 deformation, southward-verging folds and southward-directed thrusting of supracrustal
74 rocks of the northeastern North Patagonian Massif was described by Chernikoff and
75 Caminos (1996) and elaborated in a detailed structural study by von Gosen (2003), who
76 argued for Permian rather than Carboniferous crustal shortening, and possibly a
77 northeastward-directed accretionary process.

78 **FIGURE 1 ABOUT HERE**

79 However, geophysical data (Chernikoff and Zappettini, 2004; Kostadinoff et al.,
80 2005) fails to reveal any significant crustal discontinuity beneath the Río Colorado basin,
81 and the physiographical boundary of Patagonia has been moved south to the line of the
82 Huincul fault, which in its eastern part follows the Río Negro. Nevertheless, Kostadinoff et

83 al. (2005) interpret gravimetric anomalies as indicating a basement of probable Early
84 Palaeozoic age extending yet farther to the south.

85 Moreover, plate subduction and collision should result in a recognized pattern of
86 related magmatism, metamorphism and crustal melting. The original allochthonous
87 Patagonia hypothesis suffered a set-back when it was shown that supposedly
88 Carboniferous granites in the North Patagonian Massif were in fact Permian to Triassic in
89 age (Pankhurst et al., 1992). All existing collision models lack supporting magmatic
90 evidence for the postulated subduction and collision phases (i.e., subduction- and collision-
91 related granite belts, and related metamorphism, of the right age and in the right
92 relationship to the plate model).

93 We present the results of extensive study over the past six years of the ages and
94 geochemistry of igneous and metamorphic rocks that form the pre-Mesozoic basement in
95 Patagonia, and the provenance of some pre-Permian metasedimentary rocks. It must be
96 emphasized that these outcrops are very small (often only a few hundred metres in plan)
97 and sparsely distributed, due to the later extensive covering of Jurassic volcanic rocks,
98 Cretaceous–Quaternary sedimentary basins, and Tertiary basaltic lavas. Nevertheless, the
99 results, when combined with existing constraints, suggest that the North Patagonian Massif
100 was already part of Gondwana in Ordovician times. In contrast, southern Patagonia seems
101 to have belonged to an allochthonous entity that collided with the North Patagonian Massif
102 in mid-Carboniferous times as a result of *north-easterly* ocean-floor subduction. The
103 implications and consequences of this model are reviewed, especially in relation the role of
104 continental collision in the formation of the Gondwana fold belts of South America, Africa
105 and West Antarctica, as well as the distribution of Early Palaeozoic faunal provinces.
106

107 **2. Analytical methods**

108 Throughout this programme, we have dated the crystallization ages of zircon in
109 igneous and metamorphic rocks by U–Pb geochronology using SHRIMP (Sensitive High-
110 Resolution Ion Microprobe) technology at The Australian National University, Canberra
111 (Williams, 1998). The relevant data, together with precise sample localities, are presented
112 as a Supplementary Appendix to this paper, and are summarised on a sketch map of
113 northern Patagonian (Fig. 2). In addition to dating metamorphic events by analysis of
114 metamorphic overgrowths, where possible, the detrital zircons in metasedimentary rocks
115 have been dated to provide information on provenance of the protoliths. We have also
116 undertaken whole-rock geochemistry (Table 1) and Sr-Nd isotope analysis (Table 2) in an
117 attempt to constrain the tectonic environment of magmatism.

118 FIGURE 2 ABOUT HERE

119 A parallel study using conventional U–Pb zircon dating has been published recently
120 by Varela et al. (2005), in which earlier Rb–Sr and K–Ar are also reviewed (some of which
121 must now be regarded as of dubious reliability in terms of crystallization age but, as
122 pointed out by these authors, more probably relate to cooling and/or metamorphic effects).
123 As indicated by Varela et al. (2005), the main events in the evolution of Patagonia are of
124 Palaeozoic age, and metasedimentary rock units that can be ascribed to the latest
125 Precambrian are mainly restricted to the northeastern North Patagonian Massif.

126 In view of the wide time-span covered by the Palaeozoic evolution of Patagonia, it is
127 convenient to present the new results and discuss them for each of the tectonic various
128 stages that we now recognise. The time-scale used is that of Gradstein et al. (2004)

129 **3. Cambrian rifting**

130 The oldest stable area of continental basement in southern South America is the
131 2000–2200 Ma Río de la Plata craton (Santos et al., 2003). The Palaeozoic sedimentary

132 sequence of Sierra de la Ventana (also known as the Sierras Australes de Buenos Aires)
133 crops out south of the proven extent of the craton, and rests on younger (Neoproterozoic)
134 crystalline basement with crustal anatectic granite at 607 ± 5 Ma and I-/A-type granites at
135 531 ± 4 and 524 ± 5 Ma (Rapela et al., 2003). These igneous events correspond to the
136 Brasiliano/Pampean orogenic cycles of South America farther north, and may now be
137 thought of in terms of the final assembly of Gondwana (Veevers, 2005). The culminating
138 phase of igneous activity here is represented by Late Cambrian (~510 Ma) peralkaline
139 rhyolites that were derived from lithospheric mantle, and may be interpreted as recording
140 extensional tectonics related to rifting of this part of the Gondwana margin. Rapela et al.
141 (2003) suggested that this rifting episode resulted in the separation of a continental
142 fragment but could not specifically identify it within the present-day Pacific margin of
143 West Antarctica, which is a collage of small crustal blocks (see Rapela et. al., 2003, figure
144 7). However, other authors agree that a Late Cambrian passive margin was established at
145 the southern edge of Gondwana (as elsewhere, with reference to present-day geographical
146 coordinates) along the span of the subsequent Gondwanide fold belt, e.g., Curtis (2001).
147 Dalziel (1997) suggested that the rifted away portion was a large plateau area attached to
148 Laurentia and that this subsequently collided much farther to the north in the Ordovician,
149 leaving behind a fragment represented by the Argentine Precordillera.

150 **4. Ordovician magmatism**

151 In northwest Argentina, the Early Cambrian Pampean orogenic belt lies to the west
152 of the Rio de La Plata craton, and was partially overprinted by the Early to Mid Ordovician
153 Famatinian magmatic arc (Pankhurst et al., 1998, 2000), with intensive deformation in the
154 Late Ordovician. The Famatinian belt has been considered as a continental marginal arc
155 related to subduction during the approach and collision of the Precordillera terrane.
156 However, recent geochronological and structural analysis suggests that Mesoproterozoic

157 'Grenvillian' rocks exposed in the Western Sierras Pampeanas may have become part of
158 autochthonous Gondwana much earlier, being accreted to the Río de la Plata craton during
159 the Pampean event (Escayola et al., 2005; Mulcahy et al. 2005; Rapela et al. 2005a). Such
160 a continental basement, thinned during the Late Cambrian rifting, seems a likely candidate
161 for the crust underlying the Sierra de la Ventana and, perhaps, the northwestern part of the
162 North Patagonian Massif (see below).

163 FIGURE 3 ABOUT HERE

164 Previous geochronological evidence has been advanced for extension of the
165 Famatinian magmatic belt southeastwards through La Pampa province, as far as
166 Chadileuvú just north of the Río Colorado and on to the Arroyo Salado area (Fig. 1) in the
167 eastern part North Patagonian Massif (Tickyj et al., 1999; Varela et al., 1998). Our data
168 confirm these results and establish the precise contemporaneity of magmatism in these
169 areas, yielding indistinguishable Early Ordovician U–Pb SHRIMP ages of 474 ± 6 Ma and
170 475 ± 5 Ma for a (locally) early granodiorite and a late granite from Pichi Mahuida (Fig.
171 3a), 475 ± 6 and 476 ± 4 Ma for two granite bodies from the Arroyo Salado area, and 476
172 ± 6 Ma for granite at Sierra Grande 25km to the SW (Fig. 3b). Amphibolite-grade
173 metamorphism associated with the Famatinian event in the North Patagonian Massif is
174 recorded in quartzo-feldspathic gneiss from Mina Gonzalito (Fig. 4a), where new zircon
175 growth during amphibolite-grade metamorphism is dated at 472 ± 5 Ma (Pankhurst et al.,
176 2001, recalculated).

177 FIGURE 4 ABOUT HERE

178 These Ordovician granites of the North Patagonian Massif do not show signs of the
179 deformation characteristic of the contemporaneous Famatinian granites of northwest
180 Argentina, but since the latter is thought to be a direct result of the collision of the
181 Precordillera terrane, this would not be expected along the entire length of the magmatic

182 belt, and there is no evidence for terrane collision at this time in the Patagonia region.
183 Geochemical and isotopic data (Tables 1, 2) show that these are equivalent to the igneous
184 intrusions in the main part of the Famatinian belt, which are almost entirely intermediate to
185 silicic, metaluminous, with evolved initial $^{87}\text{Sr}/^{86}\text{Sr}$ ratios (0.707-0.710) and ϵNdt values
186 (-2 to -6). It is possible that the magmatism throughout the belt was initiated by post-
187 collisional lower crustal melting following the Pampean event, modified only in the
188 northern areas by further collisional compression.

189 **5. Pre-Carboniferous sedimentation**

190 The country rocks of these granites in northeastern Patagonia consists of fine-grained
191 meta-sandstones – the El Jagüelito and Nahuel Niyeu formations (see Fig. 2). González et
192 al. (2002) argue for Cambrian deposition of the former on the basis of its relationship to
193 the granites and its trace fossil content. Detrital zircons from the El Jaguelito Formation
194 (Fig. 4a) have a youngest age peak at ~535 Ma consistent with this assignment: although
195 this is strictly constraint on the maximum possible age, the dominance of this peak
196 suggests erosion from a nearby active arc and in such cases it is commonly observed that
197 the youngest detrital zircons effectively date deposition. That for the Nahuel Niyeu
198 Formation is slightly younger at ~515 Ma (both have a very few grains with even younger
199 ages that probably reflect partial Pb-loss during Ordovician granite emplacement or
200 deformation). The older provenance of both samples is typically Gondwanan with ages of
201 550–750 Ma (Pampean and Brasiliano) and ~1000–1200 Ma ('Grenvillian'), as well as a
202 small component of older ages, including some at ~2200 Ma. These patterns could relate
203 to major provenance from the areas immediately to the north in Early to Mid Cambrian
204 times, including the Río de la Plata craton (there is a very minor input of 2200-1900 Ma
205 zircons), whereas the 'Grenvillian' component is consistent with a local basement similar
206 to the Western Sierras Pampeanas as suggested above. The zircon cores from the Mina

207 Gonzalito gneiss are similar, most notably in having their main provenance at 535–540 Ma
208 (Fig. 4a), also suggesting Early Cambrian deposition and generation of the gneiss from the
209 sandstone protolith by Famatinian-age metamorphism. Thus the metapelitic rocks of the
210 northeastern North Patagonian Massif appear to have been originally deposited as
211 sediments on a continental shelf at the southern margin of Gondwana.

212 Following intrusion of the Ordovician granites, the Sierra Grande sandstone-
213 ironstone formation was deposited in Silurian or Early Devonian times (Limarino et al.,
214 1999), one of the very few such deposits known after the Precambrian era. Its probable
215 depositional environment was a quiescent platform on a stable passive margin, with no
216 volcanic input (Spalletti, 1993). The invertebrate marine fauna is of Malvinokaffric type,
217 similar to that found in the Falkland Islands. Palaeomagnetic data from this formation are
218 consistent with Permian folding, but a prior pole position consistent with stable Gondwana
219 was used to argue against it being part of a far-travelled exotic Patagonian terrane
220 (Rapalini, 1998). A sample of ferruginous sandstone from just outside the Sierra Grande
221 mine has a complex detrital zircon pattern (Fig. 4a) containing all the provenance elements
222 seen in the El Jagüelito and Nahuel Niyeu formations, as well as a youngest peak at ~500
223 Ma. This suggests sediment derivation from the same source areas to the north, but after
224 the eruption of the Late Cambrian rhyolites associated with rifting. One discordant grain
225 has an apparent age of 470 Ma, but the general absence of Ordovician zircons suggests that
226 the Famatinian granites were not exposed in the Silurian/Early Devonian source areas.

227 Thus one interpretation of the NE North Patagonian Massif is that it is underlain by
228 basement rocks that were already part of the Gondwana continent by Cambrian times,
229 perhaps thinned during the Late Cambrian rifting event, and affected by Famatinian
230 plutonism in the Early Ordovician, then becoming a largely passive margin until post-Early
231 Devonian times. Its essential integrity with the Gondwana margin in the Early Palaeozoic

232 is consistent with the observation of Kostadinoff et al. (2005) that crustal magnetic
233 signatures are continuous across the Huincul fault zone.

234 **6. Devonian magmatism**

235 FIGURE 5 ABOUT HERE

236 After the Ordovician, active magmatism reappeared at the western margin of the
237 North Patagonian Massif. Varela et al. (2005) have reported conventional ^{238}U – ^{206}Pb
238 zircon ages of 419 ± 27 Ma (MSWD = 43) and 390.0 ± 4.8 Ma (MSWD= 9) for tonalites
239 near San Martin de los Andes (Fig. 2), and of 348 ± 11 Ma (MSWD= 63, possibly
240 Carboniferous – see below) and 386.6 ± 5.4 Ma (MSWD= 9.3) for deformed leucogranites
241 cutting schists about 50 km farther to the southwest. They ascribed these to a period of
242 Devonian magmatism and migmatization associated with the Chanic orogenic event
243 identified in the areas north of Patagonia (San Rafael, Precordillera and Sierras Pampeanas
244 (Sims et al., 1998)). We have confirmed and refined the age of this magmatism in NW
245 Patagonia with U–Pb zircon SHRIMP ages of 401 ± 3 Ma for the San Martin tonalite (Fig.
246 5a) and 395 ± 4 Ma for an undeformed granite at Lago Lolog about 10 km farther north
247 (Fig. 5b). Figure 5a also illustrates ages of 371 ± 4 Ma for megacrystic granite near Gastre
248 in the southwestern North Patagonian Massif and 394 ± 4 (recalculated from Pankhurst et
249 al., 2001) for a similar megacrystic granite at Colán Conhue 300 km southeast of Bariloche
250 (Fig. 2) which, as suggested by Varela et al. (2005), may represent further extension of this
251 belt. At this stage, the lack of geochemical data for this suite precludes assignment of the
252 tectonic environment of the magmatism for the porphyritic granites, but the San Martin
253 tonalite and Lago Lolog granite have initial ϵNdt values of about -4 and Sm–Nd model
254 ages of ~ 1400 Ma (in part recalculated from Varela et al., 2005, see Table 2), consistent
255 with a Mesoproterozoic crustal component. If this belt, at least in its northwestern part,
256 represents a subduction-related arc in the west at this time, it further reinforces the

257 argument above that most of the North Patagonian Massif was autochthonous to
258 Gondwana during the Early Palaeozoic. The jump in the magmatic arc position across the
259 North Patagonian Massif after mid-Ordovician times is presumably related in some way to
260 the change of the regional tectonic scheme following collision of the Precordillera to the
261 north.

262 **7. Carboniferous subduction**

263 FIGURE 6 ABOUT HERE

264 I-type granitoids of Carboniferous to Permian age form the core of the Coastal
265 Cordillera of Chile from 33° to 38°S where they are seen in the Cordillera de Nahuelbuta
266 (Fig. 1). Southeasterly extension of this belt and its metamorphosed envelope has been
267 suggested, as far as the Piedra Santa complex near the northwestern boundary of the North
268 Patagonian Massif (Franzese, 1995), but no supporting geochronology or geochemistry are
269 available and until now it could not be traced any further. However, our results
270 demonstrate the existence of a 120 km-long belt of Early Carboniferous I-type
271 granodiorites in the eastern North Patagonian Massif, along the Cordón del Serrucho,
272 between San Carlos de Bariloche and El Maitén (41° to 42°15'S) (Fig. 2). Two samples
273 yield well-defined Early Carboniferous (~Visean) crystallization ages of 323 ± 3 and $330 \pm$
274 4 Ma; a sample of the El Platero tonalite in the Río Chico, about 50 km to the southeast,
275 gave a comparable age of 329 ± 4 Ma (Fig. 6a). A two-point conventional ^{238}U - ^{206}Pb
276 zircon age of 321 ± 2 Ma has been independently reported for a sample from the same
277 locality as MOS-043 (Varela et al., 2005). All three samples analysed, which are
278 representative of continuous outcrop, are foliated metaluminous hornblende-biotite
279 granitoids with low abundances of lithophile trace elements, rare earth element (REE)
280 patterns typical of Andinotype calc-alkaline arc rocks, positive ϵNdt values (+0.1 to +2.8),
281 and low initial $^{87}\text{Sr}/^{86}\text{Sr}$ (0.7034–0.7046) indicating a long-term light-REE depleted source

282 such as the upper mantle (Table 1). Other authors have previously suggested Carboniferous
283 magmatism in the western areas of the North Patagonian Massif, but mostly on the basis of
284 imprecise Rb–Sr whole-rock errorchrons or K–Ar geochronological data (see Varela et al.
285 2005 for a summary).

286 TABLES 1 and 2 ABOUT HERE

287 **8. Carboniferous collision-related magmatism**

288 Two previously undated granite bodies in the southwestern North Patagonian Massif
289 have yielded mid-Carboniferous (Serpukhovichian/Bashkirian) crystallization ages: 314 ± 2
290 Ma from Paso del Sapo and 318 ± 2 Ma from Sierra de Pichiñanes (Figs 2, 6b). These are
291 both peraluminous S-type garnet-bearing leucogranites with high SiO₂ contents, strongly
292 depleted heavy-REE patterns, high K₂O/Na₂O ratios, unradiogenic ϵ_{Nd} values (-5.0 to
293 -6.0 on four samples) and relatively high initial $^{87}\text{Sr}/^{86}\text{Sr}$ (0.7078–0.7098) indicative of
294 generation by upper crustal melting (Table 2). They have multistage Sm–Nd model ages of
295 ~1500 Ma that could represent the age of their deep crustal source region.

296 These results show that in the southwestern part of the North Patagonian Massif a
297 short-lived episode of subduction was followed by crustal anatexis during the mid-
298 Carboniferous. The Cordón del Serrucho runs approximately N–S (Fig. 2), but the
299 equivalence of the El Platero tonalite suggests that the arc was orientated more NW–SE,
300 and the S-type granites occur somewhat to the northeast of this trend line. Although the
301 wider distribution of I- and S-type granites in Patagonia is not clear, and the lack of
302 outcrops may unfortunately prevent further elucidation, both are typically emplaced in the
303 overriding plate above the subduction zone before and during plate collision, respectively
304 and their disposition thus strongly suggests subduction of an oceanic plate from the
305 southwest.

306 **9. Deformation and metamorphism**

307 The folded Lower Palaeozoic sequences of Sierra de la Ventana, the Cape region of
308 South Africa, the Falkland Islands (in their pre-Jurassic position off the eastern Cape) and
309 the Ellsworth Mountains of West Antarctica, consist of predominantly continental shelf
310 deposits, commencing in the mid-Cambrian, with prominent Devonian quartzite horizons,
311 and with Early Carboniferous diamictites often interpreted as of glacial origin. In the Sierra
312 de la Ventana, deformation includes intense penetrative folding and cleavage and
313 subsequent large-scale folding about approximately E–W axes, together top-to-the-
314 southwest thrusting. Prior assumptions of a Late Permian age for deformation in both the
315 Sierra de la Ventana and the Cape fold belt has been dependant on older publications of K-
316 Ar data on illite and muscovite, together with the observation that the Permian strata at the
317 top of the sequences have been deformed. However, there is notably less intense
318 deformation in the Permian shales and sandstones at the top of the sequence, which were
319 remagnetized within the fold and thrust belt, compared with the Lower Permian part of the
320 sequence, which records stronger pre-folding magnetization northeastwards towards the
321 foreland (Tomezzoli, 2001). Schematic cross-sections drawn by von Gosen et al. (1991)
322 also illustrate the more intense thrust deformation in the Curamalal and Ventana groups
323 below the level of an Early Permian unconformity. This was explained by proximity to the
324 inferred collision zone, but could alternatively indicate that deformation began before this
325 time but continued through the deposition of the Permian-to-Triassic Pillahuinco Group.
326 The general context of deformation is compressive, although in the Cape Fold Belt dextral
327 transpression is important. If resulting from a continental collision to the south of this belt,
328 the main collision must have occurred in mid-Carboniferous times, as originally postulated
329 by Ramos (1984; 1986), with less intense deformation continuing into the Permian. The
330 timing of deformation of the Palaeozoic sedimentary series in the Cape Fold Belt, Falkland

331 Islands and Ellsworth Mountains is mostly considered to be Permian in age, but this is also
332 largely based on K–Ar dating of secondary mica in folded rocks, which can only be
333 regarded as a minimum. Deformation certainly affects the Permian strata, but there is no
334 time constraint on when it began.

335 FIGURE 7 ABOUT HERE

336 Intense deformation following southward thrusting of the metasedimentary
337 basement in the northwest part of the North Patagonian Massif has been ascribed to the
338 Permian (von Gosen, 2003). However, the main constraint for the timing of deformation
339 here is the age of the Navarrette granodiorite which post-dates the thrust tectonics but was
340 affected by a late stage of NW–SE compression. We present a U–Pb zircon age of 281 ± 3
341 Ma (15 points, MSWD= 2.3) which falls well within the Early Permian (Artinskian) and
342 requires thrust tectonics to have been completed prior to this time (Fig. 7a). In the same
343 area, Basei et al. (2002) have reported a conventional U–Pb zircon age of 300 ± 6 Ma for
344 the Tardugno deformed granite, interpreted by von Gosen (2003) as a maximum age for
345 thrust tectonics.

346 Carboniferous (?) tectono-metamorphism occurred in the southern and western parts
347 of the North Patagonian Massif. Greenschist to lower amphibolite facies metamorphism
348 was attained during peak deformation, forming extensive mylonite and ultramylonite
349 ductile shear zones (Llambías et al., 2002 and references therein). As noted above, the
350 igneous rocks of the Cordon del Serrucho are strongly foliated, and are associated with
351 sheared and mylonitic schists (García-Sansegundo et al., 2005). A sample of amphibolite-
352 grade paragneiss from south of El Maitén has zircon with metamorphic overgrowths
353 recording events at 330, 340 and 365 Ma, and zircon cores with a major provenance at 440
354 Ma (Fig. 4b); it probably represents continental marginal sediments into which the
355 Carboniferous arc was emplaced. Medium-pressure, garnet-bearing metapelitic schists,

356 gneisses and migmatites of the Cushamen Formation at Río Chico (López de Luchi and
357 Cerredo, 1997), of which this is probably an equivalent, are intruded by leucogranites with
358 K–Ar muscovite ages of ~280 Ma and have been proposed as higher-grade derivatives of
359 low-grade schistose rocks at Esquel (Fig. 2) (Duhart et al., 2002). Other possibly pre-
360 Permian gneisses and migmatites are found at Río Collon Cura, where Varela et al. (2005)
361 recorded a U–Pb age of 348 ± 11 Ma, see above, and at La Potranca, south of the Río
362 Chubut, where altered orthopyroxene-garnet granulites host the S-type granite POT-316
363 (289 ± 2 Ma, Fig. 7c).

364 In contrast, the Tepuel basin in central-east Patagonia (Fig. 2, c. 43.5°S, 70.5°W) has
365 a lower section of highly deformed but low-grade Early to mid-Carboniferous
366 metasediments, dominated by diamictites and siliciclastic rocks for which glacial, epi-
367 glacial and marine environments are documented (Limarino et al., 1999). The upper
368 section, located in the western sector of the basin, is also folded and comprises a deltaic
369 sequence of conglomerates, sandstones and pelites carrying abundant Early Permian flora,
370 and also includes also restricted levels with marine invertebrates (our unpublished U–Pb
371 detrital zircon data are consistent with derivation predominantly from areas containing
372 Silurian igneous rocks, such as the Deseado Massif).

373 **10. Permian magmatism**

374 Permian (and Triassic) I-type magmatism is known from the La Esperanza area in
375 the northern part of the North Patagonian Massif on the basis of Rb–Sr whole-rock dating
376 (Pankhurst et al., 1992; Rapela et al., 1996), and recently from the western North
377 Patagonian Massif, where Varela et al. (2005) obtained ^{238}U – ^{206}Pb zircon ages of 272 ± 2
378 to 286 ± 13 Ma (albeit mostly with MSWD values of 18 to 76 that must cast some doubt
379 on the accuracy of their error estimates).

380 Our U–Pb SHRIMP results show that Early Permian granites are very extensive, in
381 both time and space, occurring across the entire width of the massif (Figs 2, 7a). The oldest
382 confirmed Permian intrusions, some of which show evidence of deformation, include the
383 ‘Tunnel tonalite’ at Rio Chico (295 ± 2 Ma, dated at 286 ± 13 Ma, MSWD= 39 by Varela
384 et al. (2005)), the Laguna del Toro granodiorite near Gastre (294 ± 3 Ma, previously dated
385 as Carboniferous by Rapela et al., 1992), a weathered two-mica granite from Piedra de
386 Aguila (290 ± 3 Ma), and leucogranite associated with migmatite at La Potranca, south of
387 the Río Chubut (289 ± 2 Ma). These may well have been generated during continued
388 deformation. They are closely followed by the Navarrette granite (281 ± 3 Ma), and a
389 muscovite migmatite west of Mamil Choique (281 ± 2 Ma). Many of these rocks, for
390 which disparate age estimates have been previously published, belong to what has been
391 denominated the Mamil Choique or Río Chico complex, once supposedly Precambrian
392 crystalline basement. Unlike the Carboniferous I-type granitoids, these characteristically
393 contain zircon inherited from the older continental crust of Gondwana, as discrete grains or
394 cores of polyphase crystals. We have not made a systematic study of the inherited
395 components, but they typically have ages of ~ 320 Ma, ~ 460 Ma, 500–650 Ma and ~ 1000
396 Ma, representing the younger part of the Gondwana spectrum, with pre-Carboniferous
397 components essentially the same as in the Cambrian metasediments of the northeastern
398 North Patagonian Massif (Fig. 7a).

399 We have re-dated samples of the granites and associated volcanic rocks from La
400 Esperanza in the northern North Patagonian Massif using the U–Pb SHRIMP zircon
401 method (Fig. 7b). As is frequently observed, the U–Pb ages are slightly older, but
402 consistent with the previously published Rb–Sr ages, with a total range of 246–275 Ma.
403 Finally, An isolated outcrop of Permian granitoid from the southeastern North Patagonian
404 Massif, the Boca de la Zanja granodiorite from near Dolavon (Fig. 2), gave 257 ± 2 Ma.

405 The younger age range for these rocks (mostly Mid to Late Permian) than for the western
406 and southern outcrops, suggest a northwesterly progression of magmatism during the
407 Permian.

408 The composition of these Permian granitoids is quite variable (Figs 8, 9), including
409 rocks of both metaluminous I-type and peraluminous S-type affinities (60–78% SiO₂), and
410 ϵNdt values range from –2 (Navarrette) to –6 (Mamil Choique), and even to –10 (for the
411 Donosa granite, La Esperanza, not dated in this study, but bracketed by the Prieto and
412 Calvo granites according to field relationships), equivalent to source model ages 1200–
413 1900 Ma. Their initial $^{87}\text{Sr}/^{86}\text{Sr}$ ratios range from 0.7036 to 0.7119. Trends in the Sr-Nd
414 isotope diagram (Fig. 9) are distinct from that exhibited by the Ordovician granitoids and
415 the Carboniferous S-type granites; whereas the latter show a shallow trend to higher initial
416 $^{87}\text{Sr}/^{86}\text{Sr}$ ratios, which is characteristic of upper crustal involvement, the Permian data
417 encompass a steeper decrease in ϵNdt values, especially in the Mid to Late Permian
418 granites of La Esperanza, that is indicative of lower crustal components. The Permian
419 intrusions thus appear to represent a major hybrid magmatic episode involving melting
420 throughout the crustal section.

421 FIGURES 8 and 9 ABOUT HERE

422 The North Patagonian Massif is thus a major site of Permian granitoid magmatism in
423 southwest Gondwana. Emplacement began in earliest Permian times (c. 295 Ma), gradually
424 moved towards the northwest during the Mid Permian, and reached a climax after the main
425 deformation of the Sierra de la Ventana fold and thrust belt. We attribute the more
426 voluminous and widespread nature of this magmatism to major access of heat to the crust
427 following break-off of the subducted slab after a continental collision that was initiated in
428 Carboniferous times. In principle it extends as far north as the rhyolite volcanism of Lihue
429 Calel in La Pampa province and Lopez Lecube syenite (258 ± 2 Ma, Fig. 7) near the Sierra

430 de la Ventana (Fig. 1), where the alkaline character of the magmatism reflects its intraplate
431 position, and continued into the Triassic (Rapela et al., 1996). These granites can be
432 identified as the most important source so far recognised for the provenance of Permo-
433 Triassic detritus in Late Palaeozoic sedimentary rocks along this part of the Pacific margin
434 of Gondwana (Hervé et al., 2003).

435 **11. Discussion: a new tectonic model**

436 The latest information on the history of magmatism, including all new data obtained
437 in this study, has been integrated with the sedimentary and tectonic record of the region
438 extending from the Gondwana margin of the Sierra Ventana to southernmost Patagonia in
439 Fig. 10. In the remainder of this section we develop our interpretation of these data in
440 terms of the separate Early Palaeozoic evolution of southern Patagonia, largely represented
441 by the Deseado Massif, and its collision with Gondwana in the mid-Carboniferous.

442 FIGURE 10 ABOUT HERE

443 Du Toit (1937) was among the first to apply the idea of continental drift to global
444 tectonics. He recognized the essential continuity of stratigraphy and deformation in the
445 Early Palaeozoic fold belts of Sierra de la Ventana in South America and the Cape region
446 of South Africa, defining his ‘Samfrau Geosyncline’. Prior to the dispersion of Gondwana
447 as separate continental fragments, these belts would have been contiguous and collinear,
448 and presumably extended to the Early Palaeozoic sequences of the Falkland Islands and the
449 Ellsworth Mountains of West Antarctica. They share, at least in part, semi-continuous
450 sedimentation from Mid-Cambrian to Permian, and have several remarkable common
451 features. With the arrival of plate tectonic theory, modern explanations of these sequences
452 and their ‘Gondwanide’ deformation were sought, falling into two groups: those in which
453 folding was ascribed to compression in a back-arc situation over a distant north-dipping
454 subduction zone (Lock, 1980; Dalziel and Grunow, 1992; Trouw and de Wit 1999, Dalziel

455 et al., 2000), and those invoking continent–continent collision (Winter, 1984; Ramos,
456 1984; 1986). Cawood (2005) has proposed that this deformation represents the final stage
457 of a long-lived ‘Terra Australis orogen’, that began in the Neoproterozoic, was developed
458 along the entire Gondwana margin of South America, East Antarctica, and southeast
459 Australia, and that was primarily accretional in nature, although this would allow for the
460 accretion of small continental terrane fragment in certain places and at various times. Since
461 the Cape Fold Belt faces the South Atlantic ocean, there is no remaining evidence of any
462 possible colliding continental mass, but the landmass of Patagonia lies to the south of the
463 Sierra de la Ventana.

464 In Figure 11, we have attempted to demonstrate a genetic connection between the
465 evidence presented above for Carboniferous–Early Permian collision in Patagonia with the
466 deformation of the Gondwanide fold belts. Continental plate reconstruction of the SW
467 margin of pre-Mesozoic Gondwana is complicated by major changes during break-up in
468 Jurassic and Cretaceous times. These include rotation and translation of fragments such as
469 the Falkland Plateau (Taylor and Shaw, 1989) and southern Patagonia (Vizán et al., 2005),
470 movements on major dextral fault zones (Rapela and Pankhurst, 1992; Jacques, 2003),
471 opening of the San Jorge and Magellanes sedimentary basins during the Cretaceous
472 (Macdonald et al., 2003; Spalletti and Franzese, in press), growth of the westernmost areas
473 by accretion of smaller terranes (Forsythe and Mpodozis, 1979), and crustal extension
474 during the emplacement of granitic batholiths (Rapela et al., 2005b). Nevertheless, most
475 recent models, e.g., Ghidella et al. (2002), concur with respect to placing the Deseado
476 Massif much closer to the southern tip of South Africa and the northern tip of the Antarctic
477 Peninsula outboard of southernmost Patagonia. These factors have been incorporated as far
478 as possible into the schematic of Fig. 11.

479 FIGURE 11 ABOUT HERE

480 We suggest that the geological data summarised in this paper for the tectonic
481 evolution Patagonia can be best explained by mid-Carboniferous collision on the southwest
482 side of the North Patagonian Massif, resulting from ocean closure by subduction towards
483 the northeast beneath an autochthonous Gondwana that included at least the greater part of
484 the North Patagonian Massif. The only possible colliding crustal block is southern
485 Patagonia, where the main exposure of Palaeozoic basement is the Deseado Massif (Fig.
486 11), which has a history of Neoproterozoic sedimentation and metamorphism followed by
487 Silurian and Devonian granite magmatism (Pankhurst et al., 2003). The strongest doubt
488 about such a collision being the main cause of deformation of the Gondwana fold belts is
489 the relatively small size of the exposed massif, but its subsurface extension to the southeast
490 is suggested by geophysical data showing the presence of an offshore basement high, the
491 Rio Chico-Dungeness Arch (Biddle et al., 1986). Even in the most recent model of
492 accretionary rather collisional orogeny (Cawood, 2005), Patagonia is recognised as
493 differing in nature from other accreted areas of the Gondwana margin, being classified as a
494 ‘peri-Gondwana continental assemblage’. Moreover, other continental basement areas in
495 the West Antarctic collage could have been involved at this stage, viz. the Antarctic
496 Peninsula, where the west coast shows evidence of Late Palaeozoic magmatic episodes
497 superimposed on older metasedimentary rocks (Millar et al., 2002). Ultimately, even if
498 overall plate kinematic readjustments Cawood (2005) were preferred in order to explain
499 Gondwana-wide folding, our evidence and arguments would still suggest that southern
500 Patagonia, perhaps together with parts of West Antarctica, was continental crust to the
501 south of the major plate boundary, so that its annexation was nevertheless an essential
502 element in the Gondwana orogeny.

503 The suture zone would lie beneath the Mesozoic sediments of the San Jorge basin.
504 The occurrence of a pre-collisional subduction-related arc and of post-collisional anatectic

505 granites in the southwestern part of the North Patagonian Massif also indicate that this was
506 the upper plate and that ocean floor was subducted northeastwards beneath this active
507 margin. The southern continental block is thus presumed to have had a passive margin, on
508 which a foreland mid-Carboniferous–Early Permian basin represented by the Tepuel Group
509 was formed before, during and after collision. Deformation was transmitted to the
510 Palaeozoic sedimentary sequences of the Sierra de la Ventana, Cape region of South
511 Africa, the Falkland Islands and the Ellsworth Mountains of West Antarctica as they were
512 forced up against the back-stop of the Río de La Plata and Kaapvaal cratons, and continued
513 into Mid Permian times. These relationships are illustrated in the schematic cross-sections
514 of Fig. 12.

515 FIGURE 12 ABOUT HERE

516 It is apparent that the colliding block could have consisted largely of continental
517 crust that rifted off from the Gondwana margin in Cambrian times, and that was formerly
518 part of the Neoproterozoic precursor of Gondwana – in tectonic terms it could be described
519 as parautochthonous rather than allochthonous. This would be consistent with the
520 occurrence of Cambrian magmatism similar to that of the Sierra de la Ventana in both the
521 Cape fold belt basement and beneath the Jurassic volcanic cover of Tierra del Fuego
522 (Söllner et al., 2000; Pankhurst et al., 2003). Separation may not have been very great
523 during the Cambrian–Carboniferous interval, which would explain the very short period of
524 subduction (no more than 20 m.y.) preceding collision.

525 Large-scale crustal melting as a result of slab break-off was also the mechanism
526 invoked by Mpodozis and Kay (1990) to explain the Permian Choiyoi magmatism, which
527 resulted in voluminous rhyolitic volcanic rocks and granites in the Frontal Cordillera and
528 the San Rafael Massif, central western Argentina, 28-35° S. These extensive volcanic
529 sequences unconformably overlie marine and continental Carboniferous and Early Permian

530 deposits (Caminos and Azcuy, 1996). Mpodozis and Kay (1990) postulated collision of an
531 unidentified exotic terrane in the west ('Terrane-X'), immediately prior to slab break-off.
532 Geological evidence for this has never been established, although there is some evidence
533 here also for Mid Carboniferous subduction-related magmatism, e.g., the Tabaquito pluton
534 (Llambías and Sato, 1995) which is affected by pre-Permian fragile deformation. We
535 suggest that an alternative to the Terrane-X hypothesis would be propagation of a
536 progressive rupture in the slab ('slab tear-off') initially induced by the relatively small-
537 scale Patagonian collision proposed in this paper. Detailed chronology of the magmatism
538 of the Choiyoi volcanism that could provide support for this idea has yet to be carried out,
539 but we note that the time-lag between the postulated collision at about 320 Ma and the start
540 of Permian magmatism is comparable to that of 20-30 m.y. observed in the Himalaya after
541 collision between India and Asia (Kohn and Parkinson, 2002).

542 **12. Consequences of the new model**

543 If the southern continental block represented by the Deseado Massif (etc.) was
544 separated from SW Gondwana from Cambrian until Carboniferous times it could be
545 expected to have a different early/mid Palaeozoic crustal history and basement evolution.
546 There are already some notable distinctions (Pankhurst et al., 2003, and Fig. 10): i.e., it
547 lacks Ordovician magmatism (although it was close to a source of Ordovician granite
548 boulders by Permian times) and instead was the site of emplacement of Silurian S-type
549 granites, which are also apparent in the detrital zircons of the Tepuel basin (our
550 unpublished data).

551 It is quite possible that Cambrian rifting south of the North Patagonian Massif
552 occurred along a pre-existing structural weakness, and thus the deep crustal structure of
553 Patagonia south of the San Jorge basin could differ in age and origin from that to the north
554 beneath the North Patagonian Massif. The recent discovery of Au mineralization

555 associated with crust-derived Jurassic rhyolites in the Deseado Massif has not so far been
556 repeated in similar rhyolites that cover the North Patagonian Massif, possibly as a result of
557 its different deep geological composition. The flora and fauna developed during the
558 Palaeozoic could also have followed significantly different evolutionary paths, depending
559 on the geographical and climatic separation of the two continental areas. The Silurian-
560 Devonian fauna of Sierra Grande in northwestern Patagonia is of Malvinokaffric type,
561 similar to that in South Africa, the Falkland Islands and Sierra de la Ventana (Müller,
562 1964; Turner, 1980, Manceñido and Damborenea, 1984), which would be easily explained
563 if this were part of the Gondwana margin at this time.

564 We conclude that mid-Carboniferous collision between continental areas represented
565 by the Deseado and North Patagonian massifs was probably responsible for initial
566 deformation of the Gondwanide fold belts, the effects of which lasted until the Mid
567 Permian. Early Permian slab-break-off resulted in voluminous granite magmatism. Further
568 tests for this model could come from examination of the few remaining unstudied pre-
569 Mesozoic rocks, from deep seismic evidence for the nature of the deep crust of beneath
570 the San Jorge basin, and further evaluation of the consequences of the model indicated
571 above.

572 **Acknowledgements.**

573 This research was started while RJP was employed by British Antarctic Survey. The major
574 part of the fieldwork and analytical programme was carried out with funding from
575 CONICET, Argentina (CONICET PIP 02082 ; ANCyT PICT 07-10735) to CWR, and a
576 Leverhulme Emeritus Fellowship (2002–2004) and NERC Small Research Grant (2004–
577 2007) to RJP. Among the numerous colleagues who have assisted in developing these
578 ideas, we especially acknowledge the help given by L.A. Spalletti and R.A. Livermore.
579 This paper is registered as NERC Isotope Geosciences Laboratory Publication No. 723.

580 **References**

- 581 Basei, M.A.S., Varela, R., Sato, A.M., Siga Jr., O., Llambías, E.J., 2002. Geocronología
582 sobre rocas del Complejo Yaminué, Macizo Norpatagónico, Río Negro, Argentina.
583 In: Cingolani, C.A., Cabaleri, N., Linares. E., López de Luchi, M.G., Ostera, H.A.,
584 Panarello, H.O. (Eds.), XV Congreso Geológico Argentino, CD-ROM, Article 152,
585 6pp.
- 586 Biddle, K.T., Uliana, M.A., Mitchum, R.M. Jr., Fitzgerald, M.G., Wright, R.C., 1986. The
587 stratigraphical and structural evolution of the central and eastern Magallanes Basin,
588 southern South America. In: Allen, P.A., Homewood, P. (Eds.), Foreland Basins.
589 International Association of Sedimentology, Special Publications 8, 41-61.
- 590 Caminos, R., Azcuy, C., 1996. Fases diastróficas neopaleozoicas. In: Archangelsky, S.
591 (Ed.), El Sistema Pérmico en la República Argentina y en la República Oriental del
592 Uruguay. Academia Nacional de Ciencias, Córdoba, Argentina (ISSN 0325-2051),
593 pp. 255-265.
- 594 Cawood, P.A., 2005. Terra Australis orogen: Rodinia breakup and development of the
595 Pacific and Iapetus margins of Gondwana during the Neoproterozoic and Paleozoic.
596 Earth-Science Reviews, 69, 249-279.
- 597 Chernikoff, C.J., Caminos, R., 1996. Estructura y relaciones estratigráficas de la
598 Formación Nahuel Niyeu, Macizo Norpatagónico oriental, Provincia de Río Negro.
599 Revista de la Asociación Geológica Argentina 51, 201-212.
- 600 Chernikoff, C.J., Zappettini, E.O., 2004. Geophysical evidence for terrane boundaries in
601 South-Central Argentina. Gondwana Research 7, 1105-1116.
- 602 Curtis, M.L., 2001. Tectonic history of the Ellsworth Mountains, West Antarctica:
603 reconciling a Gondwana enigma. Geological Society of America Bulletin 113, 939-
604 958.

605 Dalziel, I.W.D., 1997. Overview. Neoproterozoic–Paleozoic geography and tectonics:
606 review, hypothesis, environmental speculation. Geological Society of America
607 Bulletin, 109, 16-42.

608 Dalziel, I.W.D., Grunow, A.M., 1992. Late Gondwanide tectonic rotations within
609 Gondwanaland. Tectonics 11, 603-606.

610 Dalziel, I.W.D., Lawver, L.A., Murphy, J.B., 2000. Plumes, orogenesis, and
611 supercontinental fragmentation. Earth Planet. Science Letters 178, 1-11.

612 du Toit, A.L., 1937. Our Wandering Continents. An hypothesis of continental drift. Oliver
613 and Boyd, Edinburgh, 366 pp.

614 Duhart, P., Haller, M., Hervé, F., 2002. Diamictitas como parte del protolito de las
615 metamorfitas de la Formación Cushamen en Río Chico, provincias de Río Negro y
616 Chubut, Argentina. In: Cabaleri N., Cingolani, C.A., Linares, E., López de Luchi,
617 M.G., Oстера, H.A., Panarello, H.O. (Eds.), Actas del XV Congreso Geológico
618 Argentino, El Calafate, CD-ROM, Article 194, 5pp.

619 Escayola, M., Pimentel, M., Armstrong, R.A., 2005. A Neoproterozoic back-arc basin:
620 SHRIMP U–Pb and Sm–Nd isotopic evidence from the Eastern Pampean Ranges,
621 Argentina. In: Pankhurst, R.J., Veiga, G.D. (Eds.), Gondwana 12: Geological and
622 Biological Heritage of Gondwana, Abstracts, Academia Nacional de Ciencias,
623 Córdoba, Argentina, p.147.

624 Forsythe, R.D., Mpodozis, C., 1979. El archipiélago Madre de Dios, Patagonia Occidental,
625 Magallanes: rasgos generales de la estratigrafía y estructura del basamento pre-
626 Jurásico Superior. Revista Geológica de Chile 7, 13-29.

627 Franzese, J.R., 1995. El complejo Piedra Santa (Neuquén), Argentina): parte de un
628 cinturón metamórfico neopaleozoico del Gondwana suroccidental. Revista Geológica
629 de Chile 22, 193-202.

- 630 García-Sansegundo, J., Farias, P., Giacosa, R. E., Gallastegui, G., Heredia, N., 2005.
631 Structure of the North Patagonian Gondwanan basement in the Bariloche–Río
632 Chico–Pilcaniyeu area. In: Pankhurst, R.J., Veiga, G.D. (Eds.), *Gondwana 12: Geological and Biological Heritage of Gondwana, Abstracts*, Academia Nacional de
633 Ciencias, Córdoba, Argentina, p. 165.
- 635 Ghidella, M.E., Yañez, G., LeBreque, J.L., 2002. Revised tectonic implications for the
636 magnetic anomalies of the western Weddell Sea. *Tectonophysics* 347, 65-86.
- 637 González, P.D., Poiré, P.G., Varela, R., 2002. Hallazgo de trazas fósiles en la Formación
638 El Jagüelito y su relación con la edad de las metasedimentitas, Macizo
639 Nordpatagónico Oriental, provincia de Río Negro. *Revista de la Asociación Geológica Argentina* 57, 35-44.
- 641 Gradstein, F., Ogg, J., Smith, A., 2004. *A Geologic Time Scale 2004*. Cambridge
642 University Press, Cambridge, U.K., 589 pp.
- 643 Hervé, F., Fanning, C.M., Pankhurst, R.J., 2003. Detrital Zircon Age Patterns and
644 Provenance of the metamorphic complexes of Southern Chile. *Journal of South American Earth Sciences* 16, 107-123.
- 646 Jacques, J.M., 2003. A tectonostratigraphic synthesis of the sub-Andean basins; inferences
647 on the position of South American intraplate accommodation zones and their control
648 on South Atlantic opening. *Journal of the Geological Society, London* 160, 703-717.
- 649 Keidel, J., 1925. Sobre el desarrollo paleogeográfico del las grandes geológicos de la
650 Argentina. *Sociedad Argentina de Estudios Geológicos GAEA, Anales* 4, 251-312.
- 651 Kohn, M.J., Parkinson, C.D., 2002. Petrologic case for Eocene slab beak-off during the
652 Indo-Asian collision. *Geology* 30, 591-594.

- 653 Kostadinoff, J., Gregori, D.A., Raniolo, A., 2005. Configuración geofísica-geológica del
654 sector norte de la provincia de Río Negro. *Revista de la Asociación Geológica*
655 *Argentina* 60, 368-376.
- 656 Limarino, C.O., Massabie, A., Rosello, E., López Gamundi, O., Page, R., Jalfin, G., 1999.
657 El Paleozoico de Ventania, Patagonia e Islas Malvinas. In: Caminos, R. (Ed.),
658 *Geología Argentina*. Instituto de Geología y Recursos Minerales, Buenos Aires,
659 *Anales* 29, pp. 319-347.
- 660 Llambías, E.J., Sato, A.M., 1995. El batolito de Colangüil: transición entre orogénesis y
661 anorogénesis. *Revista de la Asociación Geológica Argentina* 50, 111-131.
- 662 Llambías, E.J., Varela, R., Basei, M., Sato, A.M., 2002. Deformación y metamorfismo
663 Neopaleozoico en Yaminué, Macizo Norpatagónico (40° 50´S, 67° 40´W): su
664 relación con la Fase Orogénica San Rafael y el arco de las Gondwánides. In: Cabaleri
665 N., Cingolani, C.A., Linares, E., López de Luchi, M.G., Osters, H.A., Panarello,
666 H.O. (Eds.), *Actas del XV Congreso Geológico Argentino*, El Calafate, CD-ROM,
667 Article 153, 6pp.
- 668 Lock, B.E., 1980. Flat-plate subduction of the Cape Fold Belt of South Africa. *Geology* 8,
669 35-39.
- 670 López de Luchi, M.G., Cerredo, M.E., 1997. Paleozoic basement of the southwestern
671 corner of the North Patagonian Massif: an overview. VIII Congreso Geológico
672 Chileno, Antofagasta, *Actas* 3, 1674-1678.
- 673 Ludwig, K.R., 1999. Isoplot/Ex, a geochronological toolkit for Microsoft Excel. Berkeley
674 Geochronological Center Special Publication No. 1, version 2.31, 2455 Ridge Road,
675 Berkeley, CA 94709.
- 676 Ludwig, K.R., 2000. SQUID 1.00. A user's manual. Berkeley Geochronological Center
677 Special Publication, 2455 Ridge Road, Berkeley, CA 94709.

678 Macdonald, D., Gomez-Perez, I., Franzese, J., Spalletti, L., Lawver, L., Gahagan, L.,
679 Dalziel, I., Thomas, C., Trewin, N., Hole, M., Paton, D., 2003. Mesozoic break-up of
680 SW Gondwana: implications for regional hydrocarbon potential of the southern
681 South Atlantic. *Marine Petroleum Geology* 20, 287-308.

682 Manceñido, M., Damborenea, S., 1984. Megafauna de invertebrados paleozóicos y
683 mesozóicos. In: Ramos, V. (Ed.), *Geología y Recursos Naturales de la Provincia de*
684 *Río Negro*, IX Congreso Geológico Argentino, Bariloche, Relatorio, Asociación
685 Geológica Argentina, Buenos Aires, pp. 413-466.

686 Millar, I.L., Pankhurst, R.J., Fanning, C.M., 2002. Basement Chronology of the Antarctic
687 Peninsula: recurrent magmatism and anatexis in the Palaeozoic Gondwana Margin.
688 *Journal of the Geological Society, London* 159, 145-157.

689 Mpodozis, C., Kay, S.M., 1990. Provincias magmáticas acidas y evolución tectónica de
690 Gondwana: Andes Chilenos (28-31°S). *Revista Geológica de Chile* 17, 153-180.

691 Mulcahy, S.R., Roeske, S.M., McClelland, W.C., Ellis, J.R., Nomade, S., Vujovich, G.,
692 2005. Timing and nature of forearc deformation and trenchward migration of the
693 Famatina arc during accretion of the Precordillera terrane. In: Pankhurst, R.J., Veiga,
694 G.D. (Eds.), *Gondwana 12: Geological and Biological Heritage of Gondwana*,
695 Abstracts, Academia Nacional de Ciencias, Córdoba, Argentina, p. 262.

696 Müller, H. von, 1964. Zur Altersfrage der eisenerzlagerstätte Sierra Grande, Río Negro in
697 Nordpatagonien Aufgrund Neuer Fossilfunde. *Solderd. Geol. Rundschau, Stuttgart*,
698 54, 715-732.

699 Pankhurst, R.J., Rapela, C.W., Caminos, R., Llambías, E.J., Párica, C., 1992. A revised age
700 for the granites of the central Somuncura batholith, North Patagonian Massif. *Journal*
701 *of South American Earth Sciences* 5, 321-325.

702 Pankhurst, R.J., Rapela, C.W., Saavedra, J., Baldo, E., Dahlquist, J., Pascua, I., Fanning,
703 C. M., 1998. The Famatinian magmatic arc in the southern Sierras Pampeanas. In:
704 Pankhurst, R. J., Rapela, C.W. (Eds.), The Proto-Andean Margin of Gondwana.
705 Special Publication of the Geological Society, London 142, 343-367.

706 Pankhurst, R.J., Rapela, C.W., Fanning, C.M., 2000. Age and origin of coeval TTG, I- and
707 S-type granites in the Famatinian belt of NW Argentina. Transactions of the Royal
708 Society of Edinburgh: Earth Sciences 91, 151-168.

709 Pankhurst, R.J., Rapela, C.W., Fanning, C.M., 2001. The Mina Gonzalito gneiss: Early
710 Ordovician metamorphism in northern Patagonia. Third South American Symposium
711 of Isotope Geology, Pucón, Chile, 21-24 October 2001, CD-ROM,
712 SERNAGEOMIN, Santiago, pp. 604-607.

713 Pankhurst, R.J., Rapela, C.W., Loske, W.P., Fanning, C.M., Márquez, M., 2003.
714 Chronological study of the pre-Permian basement rocks of southern Patagonia.
715 Journal of South American Earth Sciences 16, 27-44.

716 Ramos, V.A., 1984. Patagonia: ¿un continente paleozoica a la deriva? IX Congreso
717 Geológico Argentino, San Carlos de Bariloche, Actas 2, pp. 311-325.

718 Ramos, V.A., 1986. Discussion of “Tectonostratigraphy, as applied to analysis of South
719 African Phanerozoic basins” by H. de la R. Winter. Transactions of the Geological
720 Society of South Africa 89, 427-429.

721 Ramos, V.A., 2002. Evolución Tectónica. In: Haller, M.J. (Ed.), Geología y Recursos
722 Naturales de Santa Cruz. XV Congreso Geológico Argentino, El Calafate, Relatorio,
723 Asociación Geológica Argentina, Buenos Aires, pp. 365-387.

724 Ramos, V., 2004. La plataforma Patagónica y sus relaciones con la plataforma Brasileña.
725 In: Mantesso-Neto, V., Bartorelli, A., Carneiro, C.D.R., Brito-Neves, B.B. (Eds.),

726 Geologia do Continente Sul-Americano: Evolução da Obra de Fernando Flávio
727 Marques de Almeida, Beca, São Paulo, Brazil, pp. 371-381.

728 Rapalini, A.E., 1998. Syntectonic magnetization of the mid-Palaeozoic Sierra Grande
729 Formation: Further constraints on the tectonic evolution of Patagonia. *Journal of the*
730 *Geological Society, London* 155, 105-114.

731 Rapela, C.W., Pankhurst, R.J., 1992. The granites of northern Patagonia and the Gastre
732 Fault System in relation to the break-up of Gondwana. In: Storey, B.C., Alabaster,
733 T., Pankhurst, R.J. (Eds.), *Magmatism and the Causes of Continental Break-up.*
734 *Special Publication of the Geological Society, London* 68, 209-220.

735 Rapela, C.W., Pankhurst, R.J., Harrison, S.M., 1992. Triassic "Gondwana" granites of the
736 Gastre District, North Patagonian Massif. *Transactions of the Royal Society of*
737 *Edinburgh: Earth Sciences* 83, 291-304.

738 Rapela, C.W., Pankhurst, R.J., Llambías, E.J., Labudía, C., Artabe, A., 1996. "Gondwana"
739 magmatism of Patagonia: Inner Cordilleran calc-alkaline batholiths and bimodal
740 volcanic province. *Third International Symposium on Andean Geodynamics, St.-*
741 *Malo, France, Résumés étendus, ORSTOM, Paris, pp.791-794.*

742 Rapela, C.W., Pankhurst, R.J., Fanning, C.M., Grecco, L.E., 2003. Basement evolution of
743 the Sierra de la Ventana Fold Belt: new evidence for Cambrian continental rifting
744 along the southern margin of Gondwana. *Journal of the Geological Society, London*
745 160, 613-628.

746 Rapela, C.W., Fanning, C.M., Pankhurst, R.J., 2005a. The Río de La Plata craton: the
747 search for its true extent. In: Pankhurst, R.J., Veiga, G.D. (Eds.), *Gondwana 12:*
748 *Geological and Biological Heritage of Gondwana, Abstracts, Academia Nacional de*
749 *Ciencias, Córdoba, Argentina, p. 308.*

750 Rapela, C.W., Pankhurst, R.J., Fanning, C.M., Hervé, F., 2005b. Pacific subduction coeval
751 with the Karoo mantle plume: the Early Jurassic Subcordilleran belt of northwestern
752 Patagonia. In: Vaughan, A.P.M., Leat, P.T., Pankhurst, R.J. (Eds.), *Terrane Processes
753 at the Margins of Gondwana*. Special Publication of the Geological Society, London
754 246, 217-240.

755 Santos, J.O., Hartmann, L.A., Bossi, J., Campal, N., Schipilov, A., Piñeiro, McNaughton,
756 N.J., 2003. Duration of the Trans-Amazonian Cycle and its correlation within South
757 America based on U-Pb SHRIMP geochronology of the La Plata craton, Uruguay.
758 *International Geology Review* 45, 27-48.

759 Sims, J.P, Ireland, T.R., Camacho, A., Lyons, P., Pieters, P.E. Skirrow, R.G., Stuart-Smith,
760 P.G., Miró, R., 1998. U-Pb, Th-Pb and Ar-Ar geochronology from the southern
761 Sierras Pampeanas, Argentina: implications for the Palaeozoic tectonic evolution of
762 the western Gondwana margin. In: Pankhurst, R. J., Rapela, C.W. (Eds.), *The Proto-
763 Andean Margin of Gondwana*. Special Publication of the Geological Society,
764 London 142, 259-281.

765 Söllner, F., Miller, H., Hervé, M., 2000. An Early Cambrian granodiorite age from the pre-
766 Andean basement of Tierra del Fuego (Chile): the missing link between South
767 America and Antarctica? *Journal of South American Earth Sciences* 13, 163-177.

768 Spalletti, L.A., 1993. An iron-bearing wave dominated siliciclastic shelf: facies analysis
769 and paleogeographic implications (Silurian–Lower Devonian Sierra Grande
770 Formation, southern Argentina). *Geological Journal* 28, 137-148.

771 Spalletti, L.A., Franzese, J., in press. Mesozoic palaeogeography and palaeoenvironmental
772 evolution of Patagonia (southern South America). In: Gasparini, Z., Coria, R.A.,
773 Salgado, L. (Eds.), *Patagonian Mesozoic Reptiles*. Indiana University Press.

774 Taylor, G.K., Shaw, J., 1989. The Falkland Islands: new palaeomagnetic data and their
775 origin as a displaced terrane from southern Africa. American Geophysical Union,
776 Geophysical Monograph 50, 59-72.

777 Tickyj, H., Llambías, E. J., Sato, A.M., 1999. El basamento cristalino de la region sur-
778 oriental de la provincial de La Pampa: extension austral del orógeno famatiniano de
779 Sierras Pampeanas. XIV Congreso Geológico Argentino, Salta, Actas 1, 160-163.

780 Tomezzoli, R.N., 2001. Further palaeomagnetic results from the Sierras Australes fold and
781 thrust belt, Argentina. Geophysical Journal International 147, 356-366.

782 Trouw, R.A.J., de Wit, M.J., 1999. Relation between the Gondwanide orogen and
783 contemporaneous intracratonic deformation. Journal of African Earth Sciences 28,
784 203-213.

785 Turner, J.C.M., 1980. Islas Malvinas. In: Segundo Simposio de Geología Regional
786 Argentina, Academia Nacional de Ciencias, Córdoba, Argentina, pp. 1503-1527.

787 Varela, R., Basei, M.A.S., Sato, A., Siga Jr., O., Cingolani , C.A., Sato, K., 1998. Edades
788 isotópicas Rb/Sr y U/Pb en rocas de Mina Gonzalito y Arroyo Salado, macizo
789 norpatagonico atlantico, Río Negro, Argentina. X Congreso Latinoamericano de
790 Geología, Buenos Aires, Actas, 71-76.

791 Varela, R., Basei, M.A.S., Cingolani, C.A, Siga Jr., O., Passarelli, C.R., 2005. El
792 Basamento Cristalino de los Andes norpatagónicos en Argentina: geocronología e
793 interpretación tectónica. Revista Geológica de Chile, 32, 167-182.

794 Veevers, J.J. 2005. Edge Tectonics (trench rollback, terrane export) of Gondwanaland-
795 Pangea synchronized by supercontinental heat. Gondwana Research 8, 449-456.

796 Vizán, H., Somoza, R., Taylor, G., 2005. Paleomagnetic testing the behaviour of Patagonia
797 during Gondwana break-up. In: Pankhurst, R.J., Veiga, G.D. (Eds.), Gondwana 12:

798 Geological and Biological Heritage of Gondwana, Abstracts, Academia Nacional de
799 Ciencias, Córdoba, Argentina, p. 368.

800 von Gosen, W., 2003. Thrust tectonics in the North Patagonian Massif (Argentina):
801 implications for a Patagonian plate. *Tectonics* 22 (1) (2003), 1005,
802 doi:10.1029/2001TC901039.

803 von Gosen, W., Buggisch, W., Krumm, S., 1991. Metamorphism and deformation
804 mechanisms in the Sierras Australes fold and thrust belt (Buenos Aires Province,
805 Argentina). *Tectonophysics* 185, 335-356.

806 Williams, I.S., 1998. U-Th-Pb Geochronology by Ion Microprobe. In: McKibben, M.A.,
807 Shanks III, W.C., Ridley, W.I. (Eds.), *Applications of microanalytical techniques to*
808 *understanding mineralizing processes. Reviews of Economic Geology* 7, 1-35.

809 Winter, H. de la R., 1984. Tectonostratigraphy, as applied to analysis of South African
810 Phanerozoic basins. *Transactions of the Geological Society of South Africa* 87, 169-
811 179.

812

813

814 Appendix. Summary of U-Pb SHRIMP zircon analyses.

815 Attached as Excel file for supplementary publication.

816 **Figure Captions**

817 Figure 1. Sketch map of Patagonia, showing the main pre-Jurassic tectonic elements, and
818 the geographical relationship to the Sierra de la Ventana fold belt, as well as other
819 significant basement rock exposures referred to in the text. HF= Huincul fault (Chernikoff
820 and Zappettini, 2004).

821

822 Figure 2. Sketch map of the North Patagonian Massif, showing the pre-Cretaceous
823 geology, the location of analysed samples, and the results of U–Pb zircon dating presented
824 here (ages in Ma with 95% c.l. errors).

825

826 Figure 3. New U–Pb SHRIMP zircon-dating results for Ordovician granitoids: (a) from
827 Picchi Mahuida, Río Colorado (see Fig. 1), and (b) the northeastern North Patagonian
828 Massif (see Fig. 2). The data (not corrected for common Pb content) are displayed in Tera-
829 Wasserburg diagrams with 68.4% confidence limit error ellipses. The calculated age is the
830 weighted mean of ^{207}Pb -corrected ^{238}U - ^{206}Pb ages for the white ellipses: light grey ellipses
831 are for spots assumed to have suffered Pb-loss, and the dark grey ellipses are for those
832 thought to contain a significant inherited component; n = number of points in age
833 calculation/total number of areas analysed, $\pm 2\sigma$ errors, MSWD = Mean Square of
834 Weighted Deviates. The derived ages of granite intrusion in these two areas are
835 indistinguishable, and fall within the range of Famatinian granitoids in northwestern
836 Argentina.

837

838 Figure 4. (a) U–Pb zircon provenance age patterns for metasedimentary samples from NE
839 Patagonia (see Fig. 2). The curves in the main diagrams are relative probability trends
840 (Ludwig, 1999) based on the preferred age derived from individual measurements, which

841 are also shown as inset histograms. For ages less than 1000 Ma, the ^{238}U - ^{206}Pb age is used
842 after correction for initial common Pb using the ^{207}Pb measurement; for ages of 1000 Ma
843 and more, the ^{204}Pb -corrected $^{207}\text{Pb}/^{206}\text{Pb}$ age is preferred. Representative portions of the
844 cathodo-luminescence for each sample are shown on the right, with individual spot ages.
845 The Mina Gonzalito gneiss zircons have Ordovician high-grade overgrowths on complex
846 nuclei that have age patterns similar to the El Jagüelito Formation schist. (b) similar plots
847 and images for the El Maitén gneiss, which has zircon overgrowths formed during latest
848 Devonian to mid-Carboniferous amphibolite-grade metamorphism.

849

850 Figure 5. New U–Pb SHRIMP zircon-dating results for Devonian granitoids in the western
851 part of the North Patagonian Massif (Fig. 2). (a) Tera-Wasserburg diagrams for foliated
852 tonalite from San Martín de los Andes, and porphyritic granites from Cáceres (southwest
853 of Gastre) and Colán Conhue, details as in Fig. 3; (b) ^{204}Pb -corrected data plotted in a
854 Wetherill Concordia diagram for the Lago Lolog granite (since this sample contains
855 zircons very rich in U, the preferred age calculation is based on six concordant data points
856 in this diagram).

857

858 Figure 6. New U–Pb SHRIMP zircon-dating results for Carboniferous granitoids in the
859 southwestern part of the North Patagonian Massif (Fig. 2): (a) Tera-Wasserburg plots for
860 three granodiorite samples representing the Early Carboniferous subduction-related arc, (b)
861 Tera-Wasserburg diagrams for two anatectic S-type granites showing mid-Carboniferous
862 crystallization ages. Details as for Fig. 3.

863

864 Figure 7. New U–Pb SHRIMP zircon-dating results for samples representative of the
865 Permian magmatism in the North Patagonian Massif: (a) granitoid rocks with significant

866 inheritance from pre-existing Gondwana sources, including some at ~470 Ma, 500-600 Ma
867 and ~1000 Ma; PAG-257 also has inherited Carboniferous zircons, (b) the granite-rhyolite
868 complex of La Esperanza, central North Patagonian Massif. See Fig. 3 for full explanation
869 of details, (c) two small bodies from the southern part of the North Patagonian Massif.

870

871 Figure 8. Geochemical variation plots for the Carboniferous and Permian granitoids
872 analysed in this study, showing clear distinctions in petrogenesis. The Early Carboniferous
873 pre-collisional group are I-type, with lithophile-element depleted signatures and primitive
874 isotopic compositions, indicating a juvenile subduction-related source. The mid-
875 Carboniferous collisional granites are lithophile-element rich and isotopically evolved (S-
876 type), and have heavy REE depletion indicating anatexis at garnetiferous crustal depths.
877 The widespread Permian, post-collisional granites are intermediate in composition, and
878 have patterns compatible with variable hybridization of crust- and mantle-derived magmas.

879

880 Figure 9. Sr–Nd initial isotope composition plot for the Palaeozoic igneous rocks of
881 Patagonia, based on the data in Table 2. The Early Carboniferous granitoids have primitive
882 compositions largely in the long-term lithophile-element depleted quadrant, consistent with
883 a dominant mantle-derived input. All the other granitoids have evolved initial isotope
884 compositions indicating crustal contributions. Whereas the Ordovician and Carboniferous
885 S-type granites follow a shallow trend suggesting young upper crustal sources with high
886 Rb/Sr ratios, the Permian (and Triassic) granites are far more dispersed, with the steeper
887 trend for La Esperanza granites in particular indicating older, low Rb/Sr sources associated
888 with deeper continental crust. G= Mina Gonzalito gneiss, M= El Maitén gneiss.

889

890

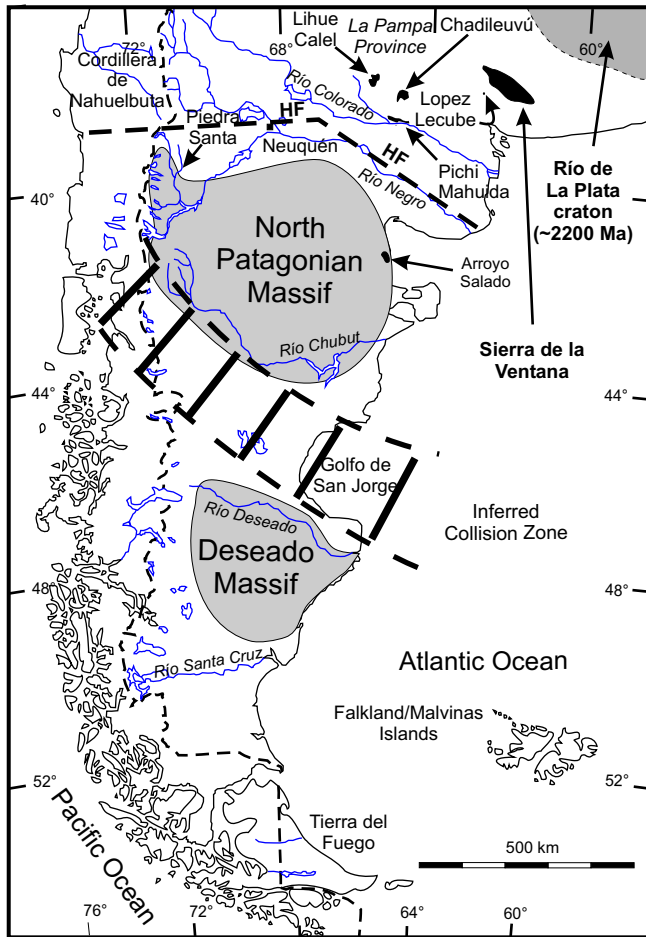
891 Figure 10. Space-time diagram showing the pre-Mesozoic sedimentary, tectonic and
892 magmatic history of the main regions of Patagonia and the adjacent Gondwana margin.
893 Crystallization ages of granitoids represented by ellipses are from the present study (errors
894 mostly included within the size of the symbols). Diamonds represent data from Basei et al.
895 (2002) and Varela et al. (2005), with vertical lines indicating 2σ error bars where
896 appropriate.

897

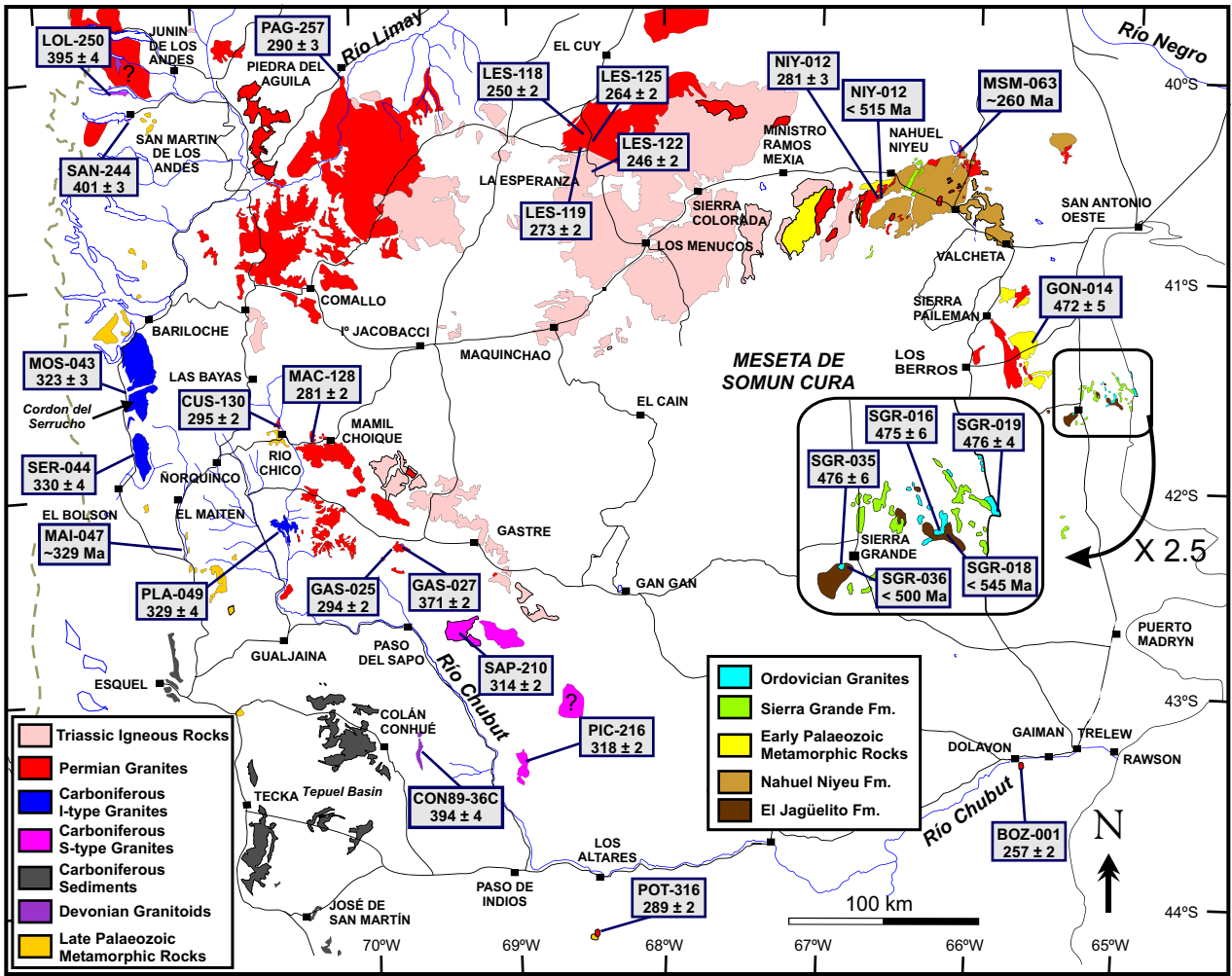
898 Figure 11 Schematic reconstruction of SW Gondwana showing Late Palaeozoic plate
899 configurations compatible with the data presented in this paper; (a) Early Carboniferous
900 subduction stage, with the North Patagonian Massif forming part of the supercontinent
901 since Ordovician (or at least Devonian) times, separated from a 'Deseado terrane' to the
902 south, the true extent of which is unknown. Coastal areas of Chile and the Antarctic
903 Peninsula consist of post-Carboniferous additions, but are shown as at the present day for
904 the purpose of easy identification. (b) Mid-Carboniferous collision stage, also showing the
905 extent of subsequent deformation on the Gondwanide fold belts and Permian granitoid
906 magmatism in the North Patagonian Massif. FI= Falkland Islands, EWM= Ellsworth–
907 Whitmore mountains crustal block.

908

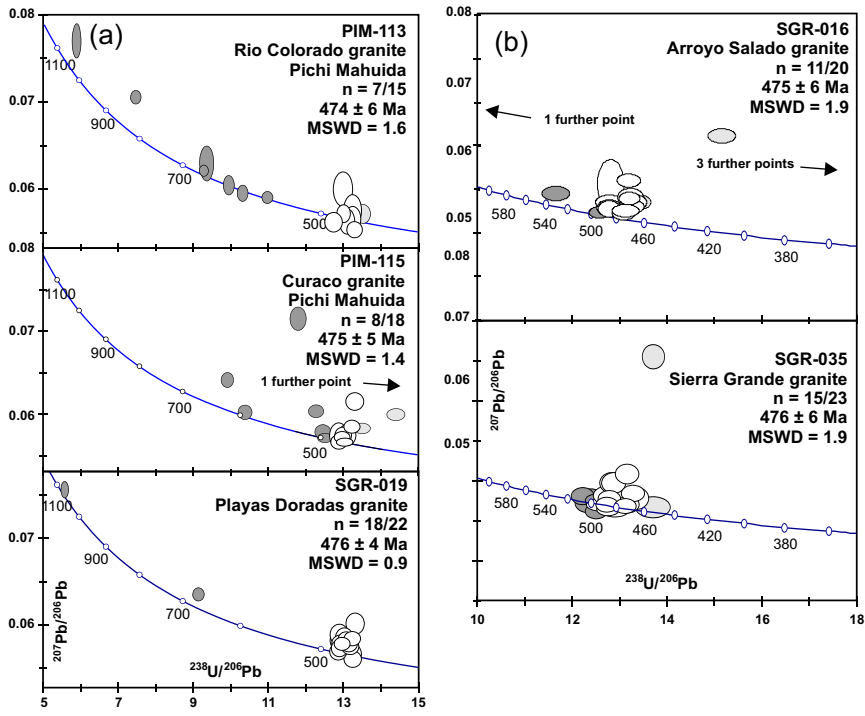
909 Figure 12. Schematic cross-sections through northern Patagonia before, during and after
910 Carboniferous continental collision according to the model advanced in Figure 11.



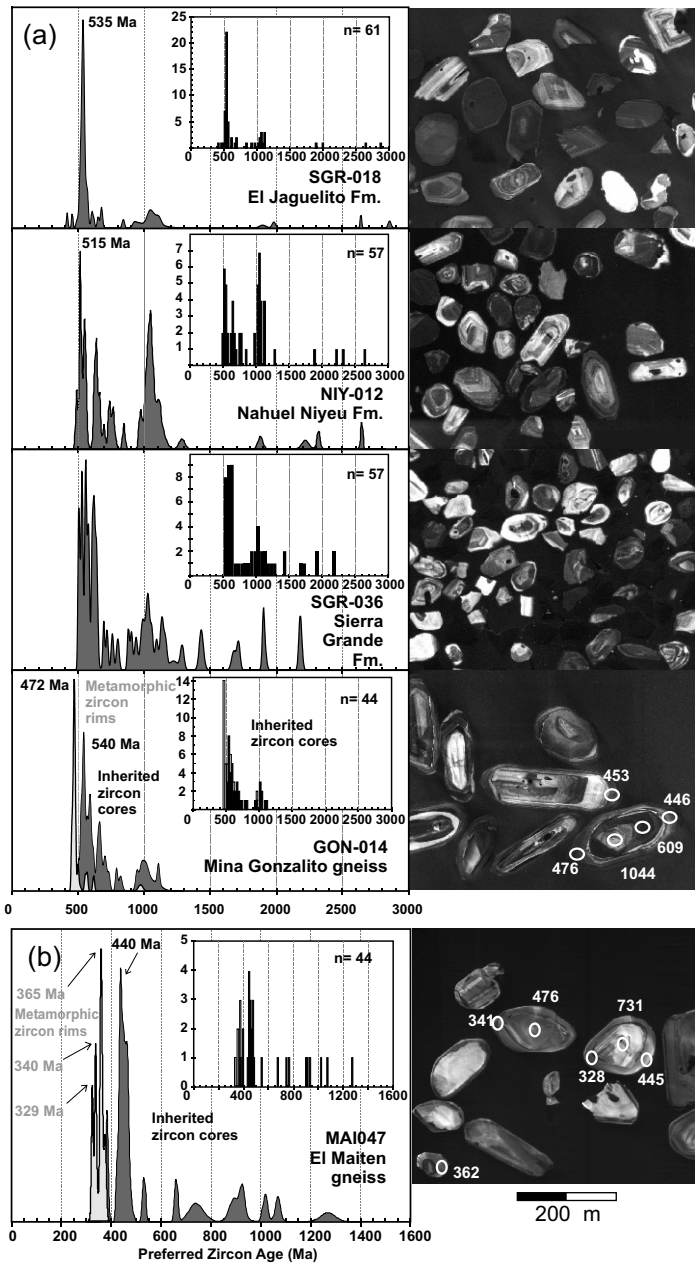
Pankhurst Fig. 1
 actual size preferred (possibly column width)



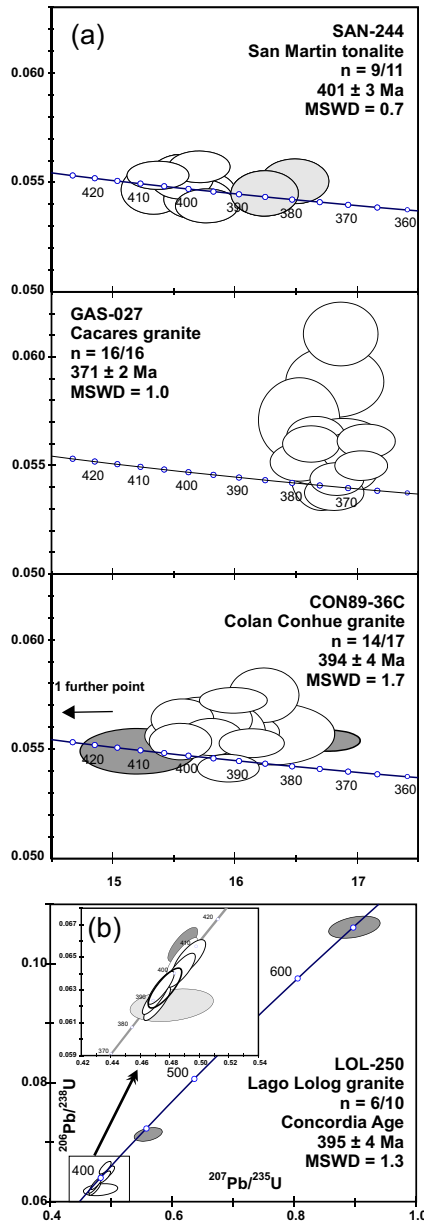
Pankhurst Fig. 2
 colour print
 full page width, or even rotated 90 degrees for larger size.



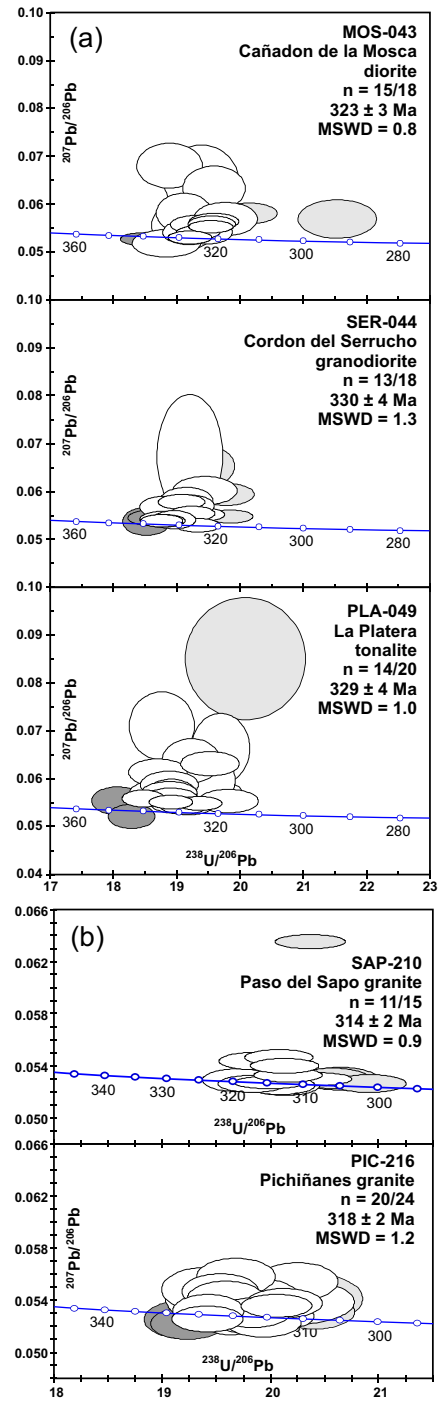
Pankhurst Fig. 3
actual size, or enlarge to page width



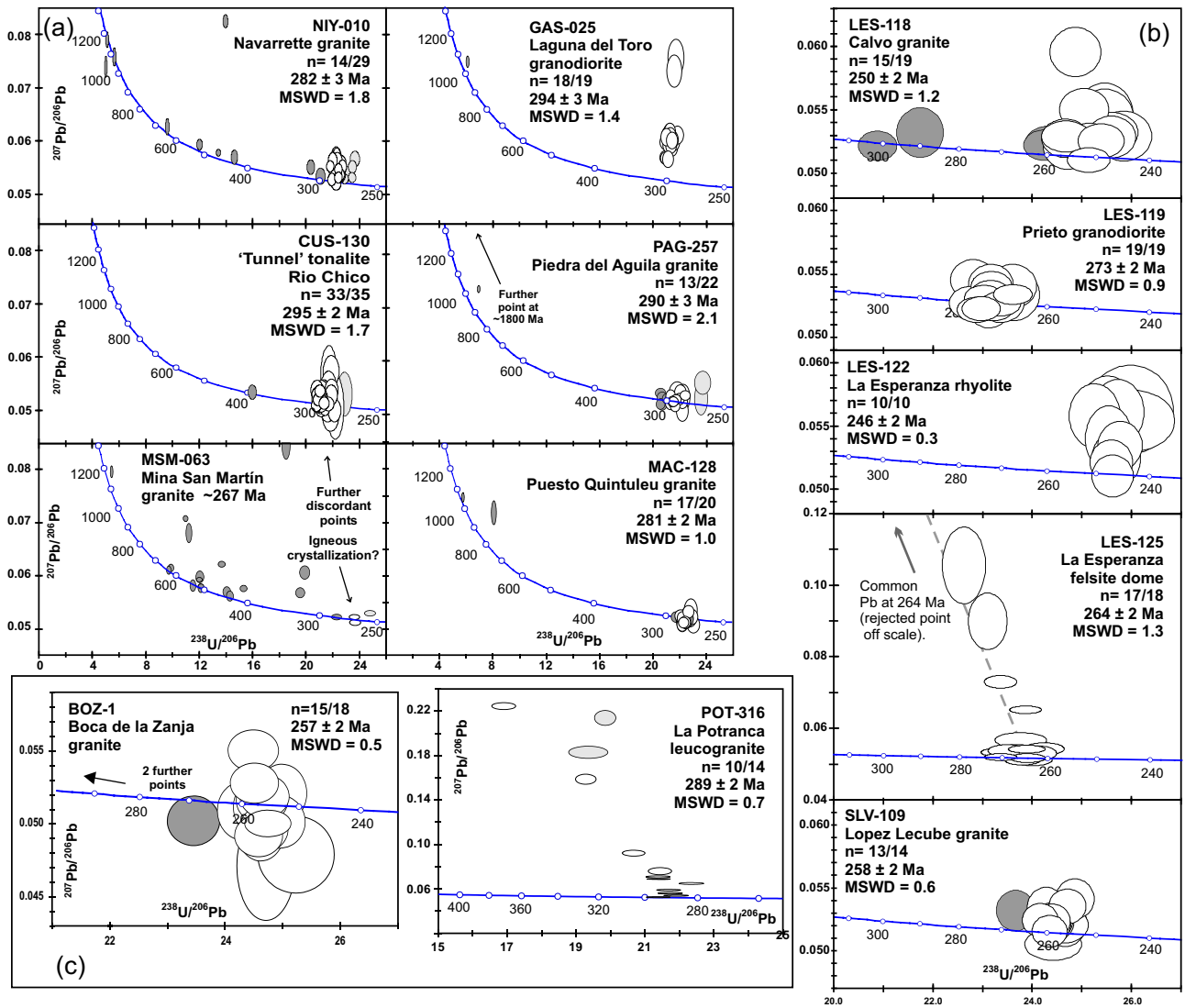
Pankhurst Fig. 4
actual size



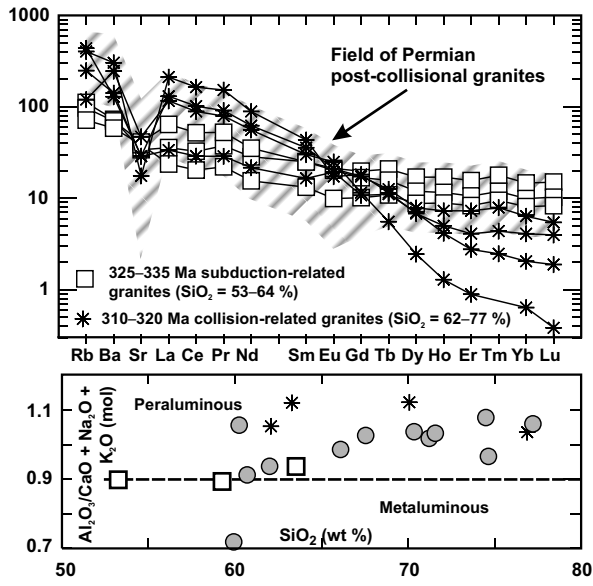
Pankhurst Fig. 5
column width



Pankhurst Fig. 6
column width



Pankhurst Fig. 7
page width



Pankhurst Fig. 8
column width